SF2A 2007
J. Bouvier, A. Chalabaev, C. Charbonnel (eds)

PLANETS AND BROWN DWARFS AROUND A-F TYPE STARS: OBSERVATIONAL RESULTS AND ACTIVITY MODELING.

M. Desort[1], A.-M. Lagrange[1], F. Galland[1], S. Udry[2] and M. Mayor[2]

Abstract. The search for extrasolar planets and brown dwarfs (BDs) making use of radial-velocity (RV) techniques has mainly focused on solar or late type stars. We have developed a new RV-measurement method allowing to detect very low mass companions around early-type stars, and we are performing a survey on a volume-limited sample of more than 200 A-F main sequence stars with SOPHIE (OHP, France) and HARPS (ESO, La Silla). This extends the planet and BD formation processes study around stars earlier than F7. We developed simulations of stellar activity (spots) to estimate more quantitatively than previously done the impact of such phenomenon on RV data and other observables (bisector, span, photometry).

1 Introduction

A general and fundamental question concerning planet formation is the impact of the mass of the central star on the formation and evolution process. The occurrence and time scale of planet formation have to be investigated and compared.

Looking for planets around early type stars is a difficult task. So far, the studies have been limited to giant stars (Sato et al. 2003, Lovis et al. 2005). These stars have small rotational velocities, but a large radius resulting in minimum possible orbital periods of the order of 100 days or slightly less. In a complementary way, to focus on main sequence stars allows us to access smaller orbital periods and to address the question of evolutionary time scales. These high-mass main-sequence stars have not been investigated so far as they exhibit fewer lines that are, in addition, generally broadened by high rotational velocities (typically 100 - 200 $\mathrm{km\,s^{-1}}$ for A-type stars). It was then thought that the radial velocity method could not be applied to those objects.

We developed a new method for radial-velocity measurements (Galland et al. 2005a) of early-type stars based on Chelli (2000). We show that planetary mass companions could be detected around those stars. We then performed radial-velocity observations of A-F type stars, using the spectrographs 1.93-m/ELODIE (Baranne et al. 2006) and 1.93-m/SOPHIE (Bouchy et al. 2006) at the Observatoire de Haute Provence (CNRS, France) in the northern hemisphere, and HARPS (Pepe et al. 2002), installed on the 3.6-m ESO telescope at La Silla Observatory (ESO, Chile) in the southern hemisphere. We present here (section 2) the results obtained so far.

Besides, it has been known for a long time that stellar activity (spots, pulsations) can also induce RV variations that can be periodic and mimic those induced by planets. Then, there might be risks of misinterpretating RV variations when they have periods shorter than or equal to the star rotational period.

In order to rule out possible stellar activity, observers have generally tried to examine either the photometric curves or the bisector variations, in addition to RV data, whenever RV variations with short periods were observed. As far as photometry is concerned, the maximum amplitude of variations in milli-magnitude is $\simeq 2.5f$ (Saar & Donahue 1997), where f (in %) is the fraction of the stellar disk covered with the spot. Depending on spot size and photometric precision, such variations may or may not be detectable. An example of the impact of these complete studies is HD 166 435 ($\simeq$ 200 Myrs, G0V), for which Queloz et al. (2001) rejected one short-period (3.8 days) planet candidate, based on bisector measurements, Ca II lines, and photometric observations.

[1] Laboratoire d'Astrophysique de l'Observatoire de Grenoble, Université Joseph Fourier, BP 53, 38041 Grenoble, France
[2] Observatoire de Genève, Université de Genève, 51 Ch. des Maillettes, 1290 Sauverny, Switzerland
[3]Based on observations made with the ESO/HARPS spectrograph at the 3.6m telescope, La Silla.

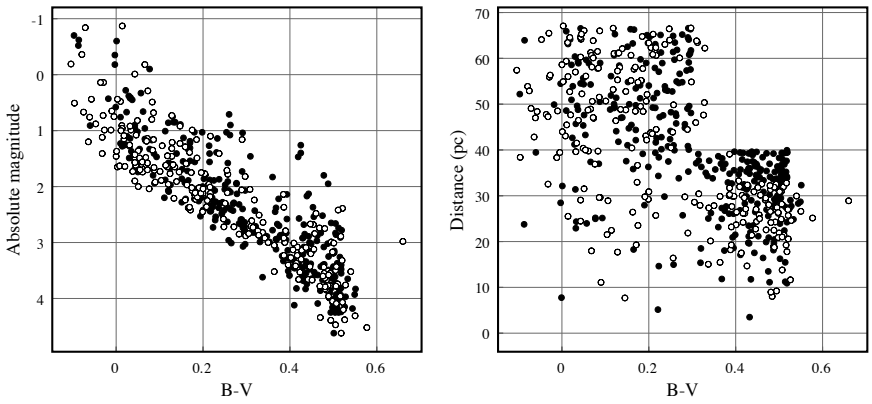

Fig. 1. Definition of SOPHIE (filled circles) and HARPS (empty circles) samples

We investigated (Desort et al. 2007) in more detail the impact of stellar spots on RV curves and on other diagnostics that are commonly used to disentangle cases of stellar activity from those of planets. We compute the visible spectra of stars with various spectral types (from F to K), projected rotational velocities and orientations, covered with one spot of different sizes and temperatures, and at different positions. We quantify the resulting RV, bisector velocity-span, and photometric variations and discuss the impact on RV studies in section 3.

2 Looking for planets around A and F type stars with radial-velocity technique: a new approach

2.1 Method

To compute the radial velocity, we use the method described in /citechelli00 (2000). Considering a reference spectrum $S_r(\lambda)$ and a Doppler shifted one, $S(\lambda) = S_r(\lambda - \lambda\frac{U}{c})$, where U is the radial velocity associated with $S(\lambda)$, we derive the cross spectrum:

$$\widehat{I}(\nu) = \widehat{S}_r(\nu)\widehat{S}^*(\nu) = \mathrm{e}^{2i\pi\nu\lambda_0\frac{U}{c}}|\widehat{S}_{\mathrm{r}}(\nu)|^2$$

The radial velocity is contained in the phase of $\widehat{I}(\nu)$. We then look for the velocity V which minimizes in a least square sense the imaginary part of the quantity: $\widehat{C}(\nu) = \mathrm{e}^{-2i\pi\nu\lambda_0\frac{V}{c}}\widehat{I}(\nu)$. The quantity to be minimized becomes:

$$\chi^2 = \sum_j \frac{Im^2[\widehat{C}(\nu_j)]}{\sigma^2(\nu_j)} = \sum_j \frac{sin^2(2i\pi\nu_j\lambda_0\frac{U-V}{c})|\widehat{S}_r(\nu)|^4}{\sigma^2(\nu_j)}$$

which is minimum when V reaches the radial velocity shift U. ν_j are discrete frequencies. The photonic radial velocity uncertainty ($\epsilon_{\mathrm{RV-Ph}}$) is simultaneously calculated using the photon noise statistic. See Chelli (2000) for further details.

Working in the Fourier space allows us to apply frequency cuts, reducing the impact of the noise (high frequencies) and of the variations of the continuum (low frequencies) due to stellar phenomena or instrumental effects. This is particularly interesting in the case of A-F type stars.

This method is fairly equivalent to the CCF one for G-K type stars, but is more suited to the case of A and F type stars with $v \sin i$ typically greater than 10-15 $\mathrm{km\,s^{-1}}$.

2.2 Sample

Our samples are volume-limited to allow statistical studies (SOPHIE 324 stars, A<67 pc, F<40 pc ; HARPS 228 stars, A<67 pc, F<33 pc) and we only selected the main-sequence A and F stars (Fig. 1). Known γ-Doradus and δ-Scuti stars have been put out of the samples.

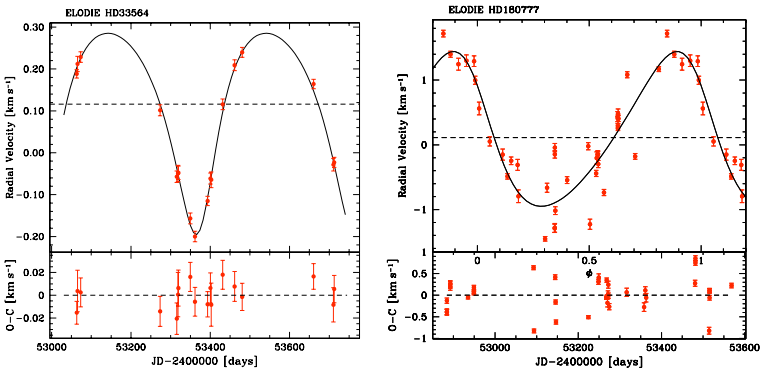

Fig. 2. Detections made with ELODIE. *left*: 9.1 M_{Jup}, $P = 388$ days around an F6V star with $v \sin i = 12\,\mathrm{km\,s^{-1}}$ (Galland et al. 2005b). *right*: 25 M_{Jup}, $P = 28$ days around a pulsating A9V star with $v \sin i = 50\,\mathrm{km\,s^{-1}}$, the residuals of the planetary fit are due to high-frequency stellar variations (Galland et al. 2006b).

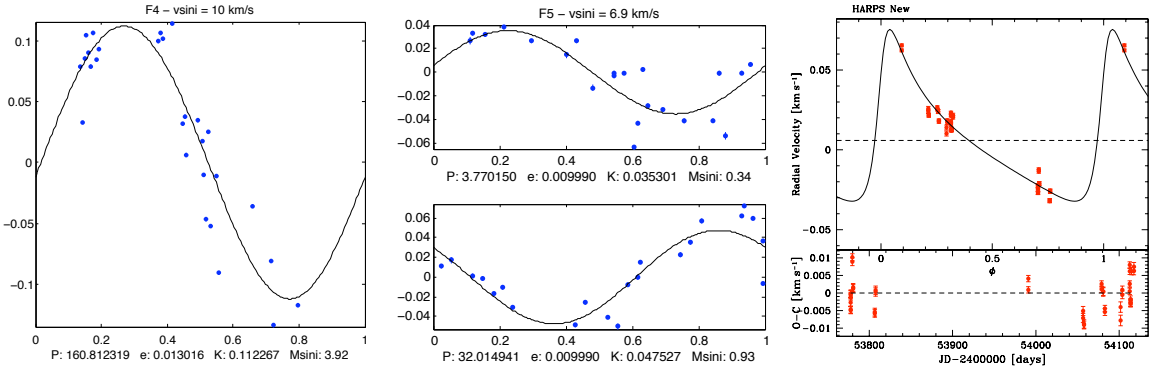

Fig. 3. Companions under characterisation with SOPHIE and HARPS. *left*: 4 M_{Jup}, $P = 160$ days around an F4V star with $v \sin i = 10$ km/s. *middle*: relatively short period around an active F5V star with $v \sin i = 7\,\mathrm{km\,s^{-1}}$, the short-period fit might be due to a stellar spot. *right*: HARPS, 1.5-3 M_{Jup}, $P = 400$-1000 days around an F4V star with $v \sin i = 8\,\mathrm{km\,s^{-1}}$.

2.3 Some results

In Figs. 2 and 3 we present some of our candidates detected with the different spectrographs used. Note that these stars sometimes exhibit high-frequency variations in addition to the planet signature, which is not surprising given their spectral type. The disentangling between both signals is made using the bisector criteria (stars with relatively high $v \sin i$; see section 3).

3 Diagnostic of stellar activity

3.1 Description of the simulations

We define the following parameters for the star: temperature $T_{\rm eff}$, gravity $\log g$, rotational velocity $v_{\rm rot}$, inclination i, metallicity [Fe/H], microturbulent velocity $v_{\rm micro}$, macroturbulent velocity $v_{\rm macro}$. We assume $v_{\rm micro} = 1.5\,\mathrm{km\,s^{-1}}$ and $v_{\rm macro} = 0.9\,\mathrm{km\,s^{-1}}$ for a G2V star, and a limb-darkening coefficient $\epsilon = 0.6$. For the spot, the free parameters are the spot colatitude θ on the star surface, the temperature $T_{\rm spot}$, and the spot size described by the parameter f_r, which is the fraction of the visible hemisphere covered by the spot[1]

[1]For a small spot ($\alpha \ll 1$) defined by its semi-angle α (2α is the angle under which the spot is seen from the star center), $f_r = 1 - \cos\alpha$. This fraction is not identical to the fraction of the projected area covered by the spot f_p on the 2D stellar disk, which is equal to $\sin^2\alpha$ for a low spot. For small values of α, we have $f_p = 2f_r$. Hereafter the spot size used is assumed to be f_r.

3.1.1 Spectrum computation

Our simulations use Kurucz models (Kurucz 1993). The 3D stellar surface is divided into longitudinal and latitudinal sections. The number of cells is tuned so that the velocity sampling is better than the resolution of the generated Kurucz spectrum. The resolution of Kurucz spectra is chosen to be twice the intrinsic resolution of the instrument we wish to simulate.

For a given set of stellar and spot properties, we first compute a synthetic spectrum using Kurucz models without rotational broadening. Then, we apply this spectrum to each cell, shifting the spectrum according to the Doppler law, taking its radial velocity into account. We then sum up the contributions of each cell, weighted by the cell's projected surface and limb-darkening, and taking the presence of a spot into account, when relevant. If a cell is covered by a spot, we use the black-body law for each wavelength of the spectrum to evaluate its weight compared to the same cell without spot (*i.e.*, at $T_{\rm spot} = T_{\rm eff}$). We generate the resulting stellar spectra at different epochs of the star's rotational phase. Typically, we take 20 epochs to cover the phase. Each spectrum is convolved with the instrumental point spread function (PSF). The spectra are computed in the range 377-691 nm, corresponding to the High-Accuracy Radial-velocity Planet Searcher (HARPS, Mayor et al. 2003) wavelength range or, in some cases, in a range corresponding only to one order of the spectrograph (see below).

3.1.2 RV, bisector, and photometric variations

We select, for each order, ranges for the spectrum that will be considered to compute the RVs and cross-correlation functions (CCFs). This selection is made so that we include neither broad lines, such as those of H or Ca, nor those from telluric origin. From these synthetic spectra, we use the method described in section 2 to derive the RVs, the CCFs, bisectors, as well as bisector velocity-spans for each order of the spectrum or for the global spectrum. The bisector shape of the lines and the resulting bisector velocity-span are estimated on the CCF in the same way as in Queloz et al. (2001). Note that, whenever we wish to compare with real data, it is possible to add noise to the spectra so as to mimic real data as closely as possible. Finally, we also derive the photometric curve over the rotational period at 550 nm.

In the following we compute the RV, bisector, and photometric variations over a wavelength range narrower than the full HARPS wavelength range (some orders were not even considered in some cases), and it corresponds to the part of the spectrum that is not affected by atmospheric lines. This choice was made in order to stick as closely as possible to the reduction of actual A-F data, presented for instance in Galland et al. (2005a,b and 2006a,b).

3.1.3 Example and comparison with observations

In Fig. 4, we show an example of comparison with real observations and the present simulations: the RV of an F7V-type star with $v \sin i = 9.6\,{\rm km\,s^{-1}}$, measured with HARPS and our software, are variable (left, top), but the profile of the CCFs changes as a function of time (left, bottom). Our simulations of the same type of star with similar $v \sin i$ show that these variations (right, top: phased) can result from the presence of a spot induced by stellar activity: we obtain the same behavior of the CCF and the same correlation between the corresponding bisector velocity-span and RV (right, bottom), with the same amplitude levels. The value of $\log R'_{HK}$ is rather high, namely -4.3, which effectively indicates a relatively high level of activity. We note that this is coherent with the high level of amplitude variations ($> 200\,{\rm m\,s^{-1}}$ peak to peak).

Figure 5 (G2V-type star, $i = 10°$, $\theta = 60°$, 1% spot, $v \sin i = 2\,{\rm km\,s^{-1}}$) shows example of results obtained when the whole spectral range is used (orders #10 to #58). We note that the features presented in Fig. 5 are identical to those expected from an orbiting planet ($0.1\,{\rm M_{Jup}}$ with a 4.4-day period). Orbiting planets produce periodic RV curves. The CCF shape does not change with time; instead, the CCFs are just shifted one to the other, consistently with a Doppler-shift of the spectra induced by the presence of a planet.

In fact, for stars with non-resolved lines (low $v \sin i$), when relatively low-amplitude periodic RV variations with short periods are observed, the bisectors are just shifted and similar to those produced in the case of a planet. Additional observables are mandatory for attributing those variations either to planets or to spots.

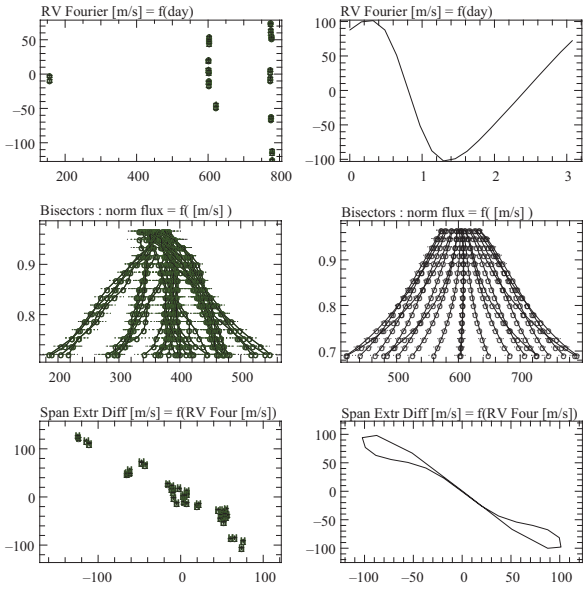

Fig. 4. Example of comparison of an active F7V-type star ($v \sin i \sim 9.6\,\mathrm{km\,s^{-1}}$) between real observations (*left*) and the present simulations (*right*): we obtain similar RV variation amplitudes (*top*), CCF behavior (*center*) and correlation between bisector velocity-span and RV (*bottom*).

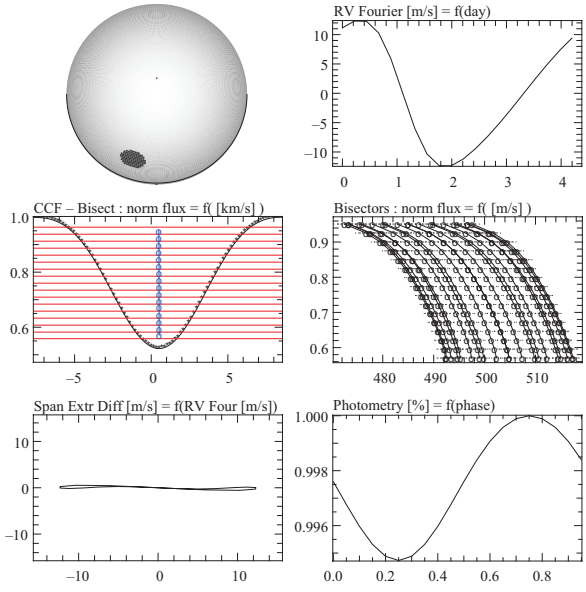

Fig. 5. Spot located at $\theta = 60°$ with a size of 1% on a G2V-type star seen almost pole-on ($i = 10°$), rotating with $v \sin i$ = $2\,\mathrm{km\,s^{-1}}$: star spot, RV curve, CCFs, bisectors, bisector velocity-span curve, photometric curve. Values measured on the whole spectrum. Part of the spectrum used: orders #10 to #58. In this case with a low $v \sin i$ value, the bisectors are only shifted, the RV curve mimics a companion, and the photometric variation is small. A Keplerian model with $0.1\,\mathrm{M_{Jup}}$ and a 4.4-day period on a circular orbit would fit the RV curve.

3.2 Impact on the search for short-period RV planets and further studies

Spots can produce a variety of features (RV, bisector shapes, and variations), whose characteristics vary according to the spots and star characteristics. The precise values of RV and, to a greater extent, the values of the bisector velocity-span depend on the line or set of lines taken into account and on the spectrograph used.

A quantitative comparison of the bisector velocity-span or bisector velocity-span to RV correlation should be made for the same line or set of lines, acquired with the same spectrograph (or at least with the same spectral resolution) and analyzed with the same software. Working on the full CCF allows individual effects to be averaged out and allows quantitative comparison to models, provided the models assume spectral types and projected rotational velocities identical to those of the star under study and use the same spectral lines and same spectral resolution.

From our studies, spots with typical sizes (1%) at the surface of stars with high $v \sin i$ will be easily identified and may be characterized using the criteria presented above (bisectors, bisector velocity-spans). In the case of stars with low inclinations and spots near the pole, confusion may however arise when the RV amplitudes are small ($< 10\,\mathrm{m\,s^{-1}}$). The situation is more complex in the case of stars with low $v \sin i$.

For stars with low $v \sin i$, spot features may, in some cases, mimic those produced by planets. This happens when 1) the observed RV variations have periods similar to the star rotational period, 2) variations are observed in the RV curves, and at the same time 3) bisectors do not change in shape, but are just shifted according to the RV changes. From the study above, this happens in the case of stars with intermediate $v \sin i$ (typ. $5\,\mathrm{km\,s^{-1}}$) and a very small (0.1%) spot or in the case of stars with low $v \sin i$ compared to the spectrograph resolution (typ. $\leq 3\,\mathrm{km\,s^{-1}}$ for a resolution of 100 000, $\leq 6\,\mathrm{km\,s^{-1}}$ for a resolution of 50 000), even with a spot that has a common (typ. $\leq 1\%$) size. When the spot is large enough and its location favorable, photometry will in general tell whether the variations are due to spots or not. In the case of small spots and for particular inclinations of the star, the photometric precision may be out of reach. Of course, the occurrence of such cases will increase when searching for planets with lower and lower masses (super-Earths or Earths) for a given orbit, as they will produce smaller RV amplitudes and bisector shapes comparable to those of smaller spots. Note that indicators of activity such as $\log R'_{HK}$ may not be sensitive enough for low levels of activity (hence the low amplitude of RV variations). Indeed, for levels of activity as low as $\log R'_{HK} \sim -4.8$, the level of the amplitude for the RV variations is still a few $\mathrm{m\,s^{-1}}$ (Santos et al. 2000, Wright et al. 2003).

The chromatic dependence of the RV amplitude may in such cases help in distinguishing between planets and stellar spots. Indeed, in the case of a planet perturbation, no such chromatic dependence is expected, whereas in the case of spots, chromatic effects will occur. This provides a possible additional criterion for testing the origin of RV variations when bisector velocity-span and/or photometric criteria cannot be applied. It has the great advantage of being an observable present in the spectroscopic data themselves.

This study has assumed a very simple case of a single spot. Of course, reality is more complex: the star may be covered by several spots with different temperatures, at different latitudes; they may also have inhomogeneities distributed in complex patterns; in addition the star may undergo complex patterns of pulsation. Simulations will be performed in the future to explore a wider variety of cases and to test more realistic cases.

References

Baranne, A., Queloz, D., Mayor, M., et al. 1996, A&A 119, 373

Bouchy F. & the SOPHIE team, 2006, in Tenth Anniversary of 51 Peg-b, Eds Arnold, Bouchy & Moutou, Publ. Frontier Group, 319

Chelli, A. 2000, A&A 358, L59

Desort, M., Lagrange, A.M., Galland, F., Udry, S., Mayor, M., 2007, A&A in press

Galland, F., Lagrange, A.M., Udry, S., et al. 2005a, A&A 443, 337

Galland, F., Lagrange, A.M., Udry, S., et al. 2005b, A&A 444, L21

Galland, F., Lagrange, A.M., Udry, S., et al. 2006a, A&A 447, 355

Galland, F., Lagrange, A.M., Udry, S., et al. 2006b, A&A 452, 709

Kurucz, R.L. 1993, CD-ROM 13, 18 http://kurucz.harvard.edu

Lovis, C., Mayor, M., Udry, S., 2005, in *Proceedings of the 13th Cool Stars Workshop*, ESA SP series 2005

Mayor, M., Pepe, F., Queloz, D., et al. 2003, The Messenger, 114, 20

Pepe, F., Mayor, M., Rupprecht, G., et al. 2002, The ESO Messenger 110, 9

Queloz, D., Henry, G. W., Sivan, J.P., et al. 2001, A&A, 379, 279

Saar, S.H., and Donahue, R.A. 1997, ApJ 485, 319

Santos, N.C., Mayor, M., Naef, D., et al. 2000, A&A 265, 272

Sato, B., Ando, H., Kambe, E., et al. 2003, ApJ, 597L, 157

Wright, J.T., Marcy, G.M., Fischer, D.A., and Butler, R.P. 2003, AAS 35, 744